Supplemental data:

Supplemental Methods:

Generation of Cter-Fgf23$^{Dmp1\text{-}cTg}$ mice overexpressing Cter-Fgf23 in osteocytes. Cter-Fgf23$^{Dmp1\text{-}cTg}$ mice harbor a targeted mutation of the Gt(ROSA)26Sor locus with a loxP-flanked STOP cassette preventing transcription of Cter-Fgf23 transgene. Cter-Fgf23 cDNA, representing the first 24 amino acids of Fgf23 (signal peptide) followed by aa 180-251 of Fgf23, is expressed following Cre-mediated excision of the STOP cassette. Briefly, a DNA fragment (Invitrogen GeneArt Gene Synthesis) containing nls-Cter Fgf23 cDNA -P2P-mCherry sequence was cloned into BstBI-MluI site by replacing the nls-Cas9-eGFP sequence of LSL-Cas9-Rosa26TV plasmid vector from Addgene (https://www.addgene.org/61408/) and further verified by sequencing. Cre-dependent knock-in targeting vector has long and short homology arms of Rosa26 locus for site specific targeting.

Tissue collection. Cortical tibia, cortical femur, bone marrow, calvaria, liver, spleen, kidney, and heart were collected at necropsy for RT-qPCR, blots, and immunohistochemistry. The blood was spun in dry tubes and serum stored at -80^{o}C for biochemistry to the exception of a fraction mixed to anti-coagulant EDTA allowing complete cell blood count (CBC) using a hematology analyzer (Hemavet 950, Drew Scientific, Erba diagnostics, Miami, FL, US).

Biochemistry. FGF23 transcription and cleavage can be assessed non-invasively in vivo by using two different commercially available assays (Quidel): the C-terminal FGF23 assay (cFGF23), which captures both iFGF23 and Cter-FGF23, and is considered a measure of total FGF23, and the iFGF23 assay, which exclusively detects intact hormone.[69] The ratio between iFGF23 and cFGF23 is used as a surrogate marker for FGF23 cleavage.[12,38,39] Serum iron and unsaturated iron-binding capacity (UIBC) were assessed using available assays (Pointe Scientific #I7504-60). Total iron-binding capacity (TIBC) was calculated as the addition of serum iron with UIBC, and transferrin saturation (TSAT) as serum iron divided by TIBC. Hepcidin (Life Science #HMC-001), BMP2 (Abcam #ab119582), and BMP9 (Sigma-Aldrich RAB1118) were measured in serum and supernatants.

RNA isolation, RT-PCR, and RNA sequencing. We isolated total RNA from tissues and from cell cultures using TRI reagent (Waltham, MA, USA) and purified RNA using RNeasy kit (Qiagen, Germantown, MD, USA).

For RNA sequencing, we isolated RNA from livers of WT and Cter-Fgf23$^{Dmp1\text{-}cTg}$ mice 6 hours post-injection with mouse recombinant IL-1β or saline solution. The total RNA library for each

individual sample was prepared using the TruSeq Total RNA-Seq Library Preparation Kit (Illumina, San Diego, CA), and the bar-coded cDNA libraries were sequenced for 150 bp paired end reads using Illumina NextSeq to generate 30-40 million reads/sample. Reads from each library were mapped to the mouse transcriptome and genome, filtered using StrandNGS software suite (Strand Life Sciences, Bangalore, Karnataka, India), following Strand alignment and filtering pipelines. Reads were normalized using DESeq and we used baseline transformation to the median for each sample. Fold-change (FC) and p value were calculated using moderated T-test and data were used for subsequent downstream pathway analyses using the Ingenuity Pathway Analysis platform (IPA, Qiagen, Redwood City, CA). FastQ files and processed RNAseq data were submitted to GEO repository under the accession number GSE227268.

For RT-PCR, we synthesized first-strand cDNA (iScript cDNA Synthesis Kit, Bio-Rad Laboratories, Hercules, CA) and used the iCycler iQ real-time PCR detection system, iQ SYBR Green supermix (Bio-Rad Laboratories, Hercules, CA), and adequate primer pairs for real-time quantitative PCR analysis. Primer sequences are provided in **Supplemental Table 1**. The threshold of detection of each gene expression was set at optimal reaction efficiency. The expression was plotted against a standard dilution curve of relative concentration, normalized to 60S ribosomal protein L19 (*Rpl19*) expression in the same sample, and expressed as fold change versus respective controls.

Immunoprecipitation, WB and Mass Spectrometry

Serum samples were immuno-precipitated from 300 µL of serum using Dynabeads bound to goat anti-FGF23 antibodies recognizing Cter domain of iFGF23. Proteins were separated by electrophoresis on 4-12 Bis-Tris minigels (NP0335, Invitrogen), transferred on 0.22 PVDF membranes (Bio-Rad Laboratories) and probed with goat polyclonal anti-FGF23 (Immutopics). Antigen antibody complexes were visualized by immunoblotting using anti-goat and anti-rabbit IR fluorescent antibodies using the Azure 600 (Azure Biosystems, Dublin,CA).

Fgf23^{KO} derived osteoblasts were treated for 2 hours either with Cter-FGF23 or with iFGF23, and immunoprecipitated using Dynabeads and goat anti-Cter-FGF23 antibodies. Tandem mass spectra were extracted by mass spectrometry, at NU Core following ingel protein digestion using trypsin. All MS/MS samples were analyzed using Mascot (Matrix Science, London, UK; version 2.5.1). Mascot was set up to search the SwissProt_2018_02 database (selected for Mus musculus) for tryptic peptides. Mascot was searched with a fragment ion mass tolerance of

0.050 and a parent ion tolerance of 10.0 PPM. Scaffold (version Scaffold_5.0.1, Proteome Software Inc., Portland, OR) was used to validate MS/MS based peptide and protein identifications. Peptide identifications were accepted if they could be established at greater than 95.0% probability by the Peptide Prophet algorithm.[70] Protein identifications were accepted if they could be established at greater than 99.0% probability and contained at least 2 identified peptides. Protein probabilities were assigned by the Protein Prophet algorithm.[71] Proteins that contained similar peptides and could not be differentiated based on MS/MS analysis alone were grouped to satisfy the principles of parsimony.

Recombinant proteins

To test the in vivo effect of inflammation, 6 week-old C57BL/6J male mice (Jackson Laboratory) were injected intra-peritoneally with 50 or 250 ng/g of mouse recombinant IL-1β, (Cell Signaling Technology, Danvers, MA, US), 3.5×10^6 particles of heat-killed Brucella abortus (BA) strain 1119 (National Veterinary Services Laboratories) or saline control as previously described. All animals not treated with IL-1β or BA received an equivalent volume of saline solution. Recombinant mouse proteins BMP2, BMP6, and BMP9 were obtained from R&D Systems (355-BM-050, 6325-BM-020, 5566-BP-010, respectively) and injected ip in WT mice at 10 ng/g of body weight and at 10 ng/mL in culture medium. C-ter-FGF23 was produced in HEK cells at Northwestern Protein Core and used at 50 ng/g of body weight in mice and at 50 ng/mL in culture. FGF23 cleavage was blocked in osteocytes using an irreversible furin/furin-like pro-protein convertase inhibitor 15 μg/mL (EMD Millipore, MA, USA).

Primary cell culture

Primary bone marrow stromal cells (BMSC) and primary osteocytes were collected from 6 weeks-old male mice. Bone marrow was isolated by centrifugation and primary osteoblasts were isolated from cortical bone fragments after successive trypsin collagenase digestions. Cells were plated for 21 days in osteogenic differentiation medium: minimum essential medium (Thermo Fisher Scientific 10-022-CV) with 10 % fetal bovine serum (Corning 35-010-CV), 1 % penicillin-streptomycin (Thermo Fisher Scientific 15140-022), 10 mM beta glycero-phosphate and 50 mg/L ascorbic acid (Sigma Aldrich G9422 and A8960, respectively).

Luciferase assay

MC3T3-E1 cells were transfected with a secreted luciferase under the control of the 1.5 kDa promoter of *Fgf23* sequence. Cells were plated in 24-well plates for 21 days in osteogenic

differentiation medium and treated for 24 hours with IL-1β. Supernatants were collected after 24 hours of treatment and the activity of the luciferase reflecting *Fgf23* promoter activity was determined using a luminescence assay (LF033, GeneCopoeia).

Supplemental Table 1: Sequences of primers used for RT-PCR

Gene	Forward Sequence	Reverse Sequence
Rpl19	GCC CAC AAG CTC TTT CCT TTC G	GTG TTT TTC CGG CAA CGA GC
Fgf23	CAC TGC TAG AGC CTA TCC	CAC TGT AGA TGG TCT GAT GG
Galnt3	CGA CGT CCG CGA GAG ACC CT	GGG GCG GGC AGC GCT TAA AT
Fam20c	GCC AAG TTG TTT GAG CAC CC	TTC ATG CGG CCA GTC AGG AT
Pcsk1	CTT GCT TCT TTT CTC CCA GCC C	TGT TGT TCA GCC CAC GTC A
Pcsk2	TTT GGA GTC CGA AAG CTC CC	TTG CCC AGT GTT GAA CAG GT
Furin	AGG ATC TGG CCC TTA CCC TGT	AGC CAC TTT ACT TGA GGC TCC
Pcsk4	TGT GAC GGC TAC ACC AAC AG	ATA ATG GTG GCT CAC TTG GCG
Pcsk5	CTG CGA GGA TGG ACA GTT CT	CTC TTC CGT AGC ATC CTT GC
Pcsk6	GAG TAC ACA GCT CCT TCC ATC C	CAC ATC CCT TAT GGC AGC GA
Pcsk7	TCG GAT ATA CGG GGG ACC AT	TCC TGG CCT GGG TAA CCA TA
Pcsk8	GAA TTC GGC CCC TGC CTA GT	GGG GCT TCT CTC ATT GAG GC
Pcsk9	GTG GGT ATA GCC GCA TCC TC	CTC CGA TGA TGT CCT TCC CG
Hamp	ATG ATG GCA CTC AGC ACT CG	AGG ATG TGG CTC TAG GCT ATG
Bmp2	GTC CCT CGG ACA GAG CTT TT	AAC ACT AGA AGA CAG CGG GTC
Bmp6	GGG CAC TCT TTC AGG TTC CA	AAA TGA CGG CTA CGG CAG AT
Bmp9	CTG GGA TTG TCT GGA GCT GG	CCA TCC TTC GTC CCG AAT GT
Erfe	GGA TCT ACT ACC TGC CCG AAG	TCA CAG GCC CAG GAG GAT AG

Supplemental Figure Legends

Supplemental Videos: Time lapse microscopy of MC3T3-E1 osteoblasts stably transfected with a vector producing a double-tagged FGF23 (RFP at the N- and GFP at the C-terminal domain) under the control of *Fgf23* 1.2 Kb promoter and treated with saline or IL-1β with a time frame acquired every 60 minutes for 24 hours (A-B). Higher magnification and time frame taken every 10 minutes for 2 hours (C).

Supplemental Figure 1: Acute inflammation increases bone FGF23 protein secretion in vivo. Supernatant A) cFGF23 and B) iFGF23 in 24 hours organ cultures isolated from 6 week-old WT mice and treated with 10 ng/mL IL-1β. Supernatant C) cFGF23 and D) iFGF23 in 24 hour organ cultures isolated from 6 week-old WT mice 6 hours post in vivo treatment with 250 ng/g IL-1β. n≥3/group, $p<0.05$ vs. (a) Ctr.

Supplemental Figure 2: Body weight and neutrophil count in WT and *Fgf23*$^{Dmp1\text{-}cKO}$ mice in acute inflammation. A) Body weight and B) neutrophil count in 6-week-old WT and *Fgf23*$^{Dmp1\text{-}cKO}$ mice 6 hours post administration of a single dose of 250 ng/g IL-1β. n≥5/group, $p<0.05$ vs. (a) WT Ctr, (b) WT IL-1β.

Supplemental Figure 3: Effects of acute inflammation on mRNA expression of Pcsk proteases. mRNA expression of A-B) *Pcsk 1* and *2*, C) *Pcsk3* (*Furin*), D-I) *Pcsk 4* to *9* in 6 week-old WT mice 6 hours post-treatment with 250 ng/g IL-1β. n≥3/group, $p<0.05$ vs. (a) Ctr.

Supplemental Figure 4: Effects of acute inflammation in *Furin*$^{Dmp1\text{-}cKO}$ mice. A) Neutrophil count, B) osseous *Furin* mRNA expression, C) serum phosphate, D) urine phosphate, E) hemoglobin (Hb) levels and F) bone marrow *Erfe* mRNA expression in 6-week-old WT and *Furin*$^{Dmp1\text{-}cKO}$ mice 6 hours post administration of a single dose of 250 ng/g IL-1β. n≥5/group, $p<0.05$ vs. (a) WT Ctr, (b) *Furin*$^{Dmp1\text{-}cKO}$ Ctr, (c) WT IL-1β.

Supplemental Figure 5: Cter-FGF23 peptides attenuate hepcidin secretion independently of ERFE/BMP6.

Serum A) cFGF23, B) iFGF23, C) i/cFGF23, D) phosphate, E) hepcidin, F) iron, G) TSAT in 6-week-old WT and *Fgf23*$^{Dmp1\text{-}cKO}$ mice 6 hours post administration of a single dose of 3.5×10^6 particles of heat-killed Brucella abortus strain 1119. n≥5/group, $p<0.05$ vs. (a) WT-Ctr, (b) *Fgf23*$^{Dmp1\text{-}cKO}$ Ctr, (c) IL-1β WT. H) Bone marrow *Erfe* mRNA expression in 6-week-old WT mice 6 hours post administration of a single dose of 50 ng/g Cter-FGF23. n≥4/group. *Bmp6*

mRNA expression in I) selected organs, and time course of J) liver *Bmp6* mRNA in 6-week-old WT mice up to 6 hours post administration of a single dose of 250 ng/g IL-1β. K) Liver *Hamp* mRNA expression and serum L) hepcidin, M) iron and N) TSAT and O) phosphate in 6-week-old WT mice implanted with gelatin sponges containing MC3T3-E1 cells transfected with an empty (Ctr) or a Cter-FGF23 vector, 6 hours post administration of a single dose of 50 ng/g BMP (2, 6 or 9). n≥5/group, p<0.05 vs. (a/*) Ctr, (b) Ctr Cter-FGF23, (c) Ctr BMP (2, 6, 9). Serum P) cFGF23, Q) iFGF23, R) i/cFGF23, S) hepcidin in 6-week-old WT and *Cter-Fgf23*$^{Dmp1\text{-}cTg}$ mice 6 hours post administration of a single dose of 10 ng/g BMP (2 or 9) or saline. n≥4/group, p<0.05 vs. (a) WT-Ctr, (b) *FGF23*$^{Dmp1\text{-}cTg}$ Ctr, (c) WT-BMP (2 or 9).

Supplemental Figure 6: Effects of acute inflammation in *Cter-Fgf23*$^{Dmp1\text{-}cTg}$ mice.

Serum A) cFGF23, B) iFGF23, C) i/cFGF23, D) phosphate, E) $1,25OH_2D$, F) hepcidin, G) iron, H) TSAT, I) hemoglobin and J) Heatmap-represented expression of hepatic genes identified in the SMAD/BMP differentially regulated pathway in *Cter-Fgf23*$^{Dmp1\text{-}cTg}$ liver extracts vs. WT in 6-week-old WT and *Cter-Fgf23*$^{Dmp1\text{-}cTg}$ mice 6 hours post administration of a single dose of 250 ng/g IL-1β. n≥4/group, p<0.05 vs. (a) WT Ctr, (b) *Cter-Fgf23*$^{Dmp1\text{-}cTg}$ Ctr (c) WT IL-1β.

Figure S1

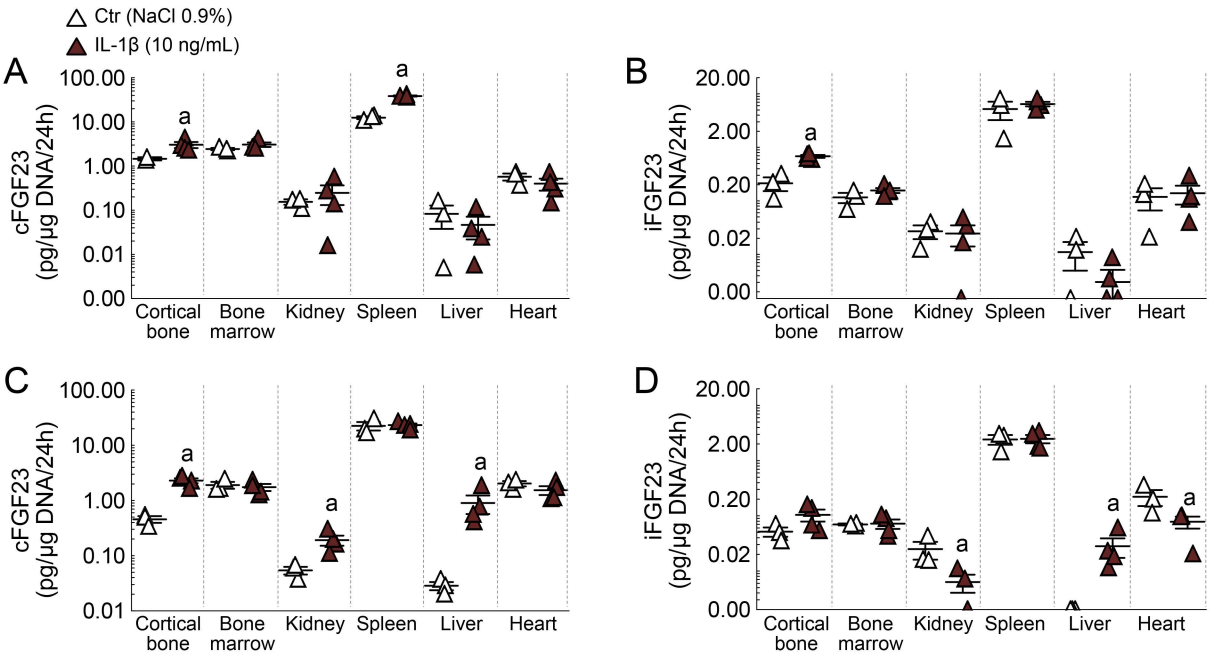

Ctr (NaCl 0.9%)
IL-1β (10 ng/mL)
A
cFGF23 (pg/µg DNA/24h)
100.00
10.00
1.00
0.10
0.01
0.00
a
a
Cortical bone
Bone marrow
Kidney
Spleen
Liver
Heart
B
iFGF23 (pg/µg DNA/24h)
20.00
2.00
0.20
0.02
0.00
a
C
cFGF23 (pg/µg DNA/24h)
100.00
10.00
1.00
0.10
0.01
a
a
a
D
iFGF23 (pg/µg DNA/24h)
20.00
2.00
0.20
0.02
0.00
a
a
a

Figure S2

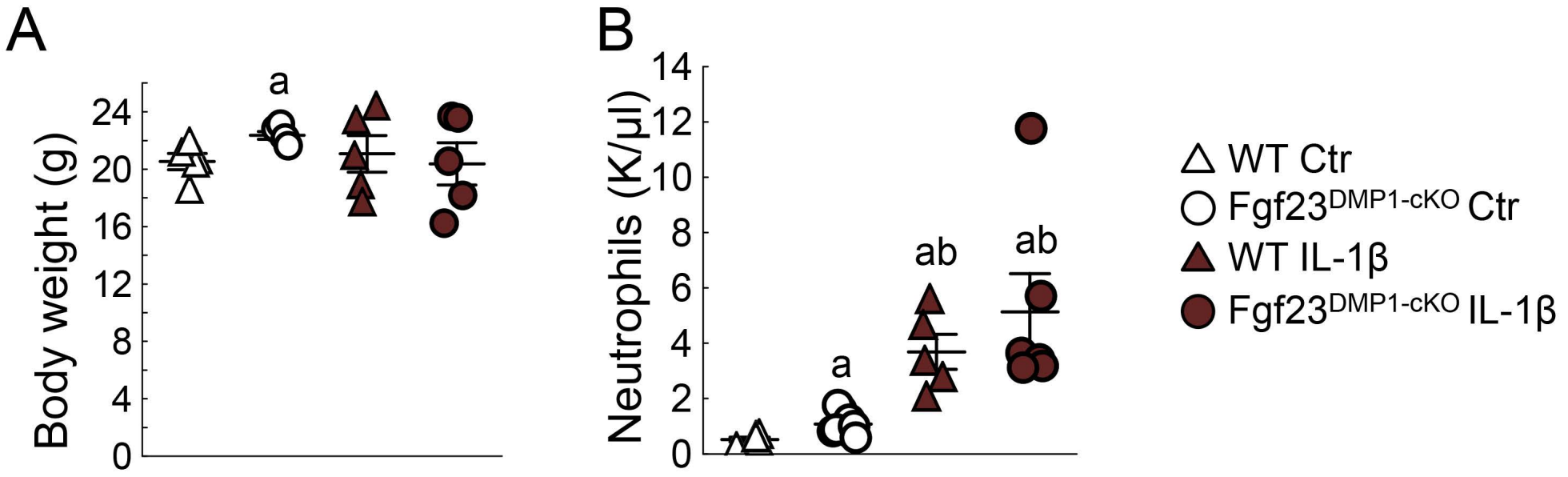

A
Body weight (g)
0
4
8
12
16
20
24
a
B
Neutrophils (K/µl)
0
2
4
6
8
10
12
14
a
ab
ab
WT Ctr
Fgf23DMP1-cKO Ctr
WT IL-1β
Fgf23DMP1-cKO IL-1β

Figure S3

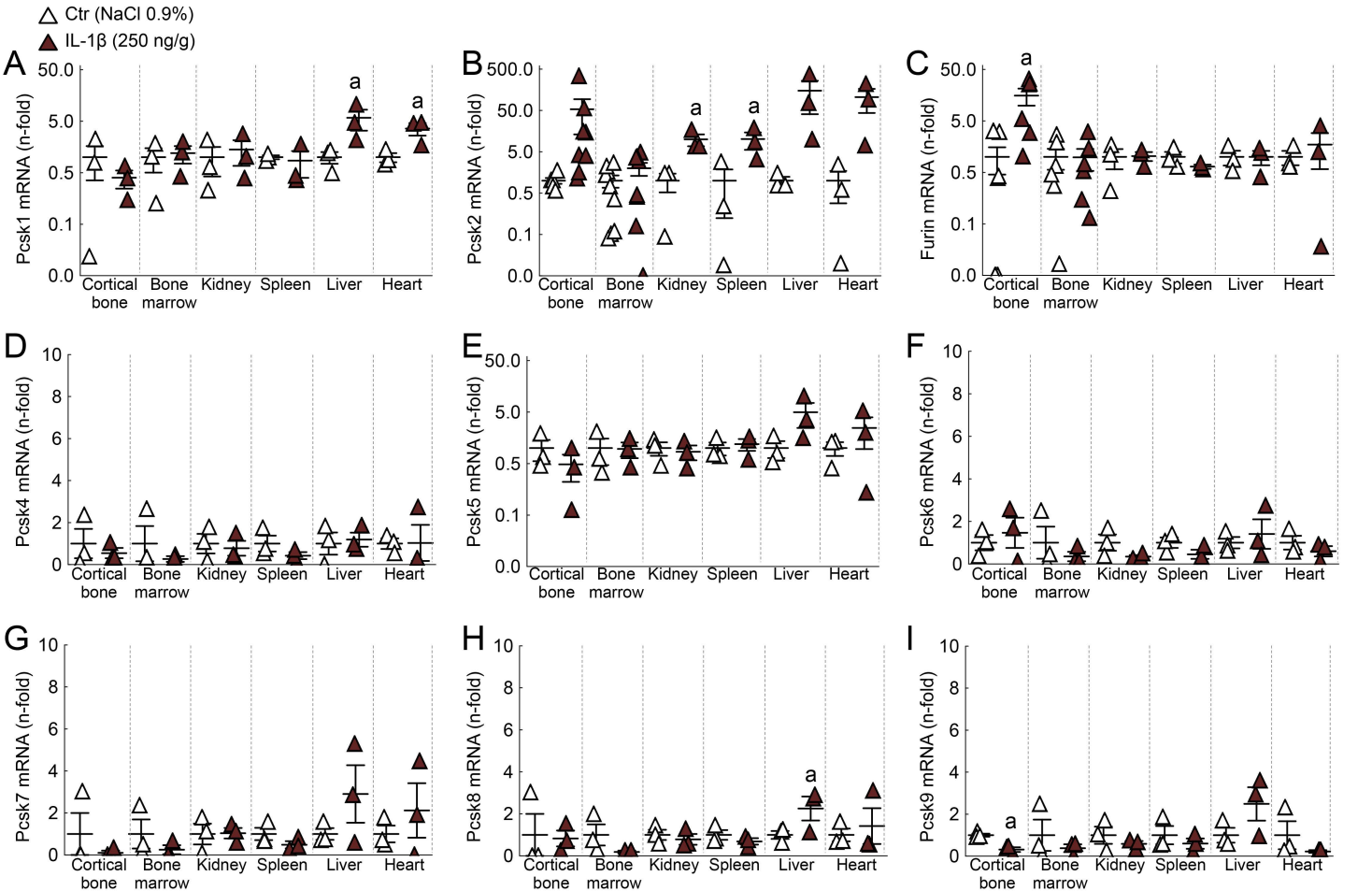

Ctr (NaCl 0.9%)
IL-1β (250 ng/g)
A
Pcsk1 mRNA (n-fold)
B
Pcsk2 mRNA (n-fold)
C
Furin mRNA (n-fold)
D
Pcsk4 mRNA (n-fold)
E
Pcsk5 mRNA (n-fold)
F
Pcsk6 mRNA (n-fold)
G
Pcsk7 mRNA (n-fold)
H
Pcsk8 mRNA (n-fold)
I
Pcsk9 mRNA (n-fold)
Cortical bone
Bone marrow
Kidney
Spleen
Liver
Heart
a

Figure S4

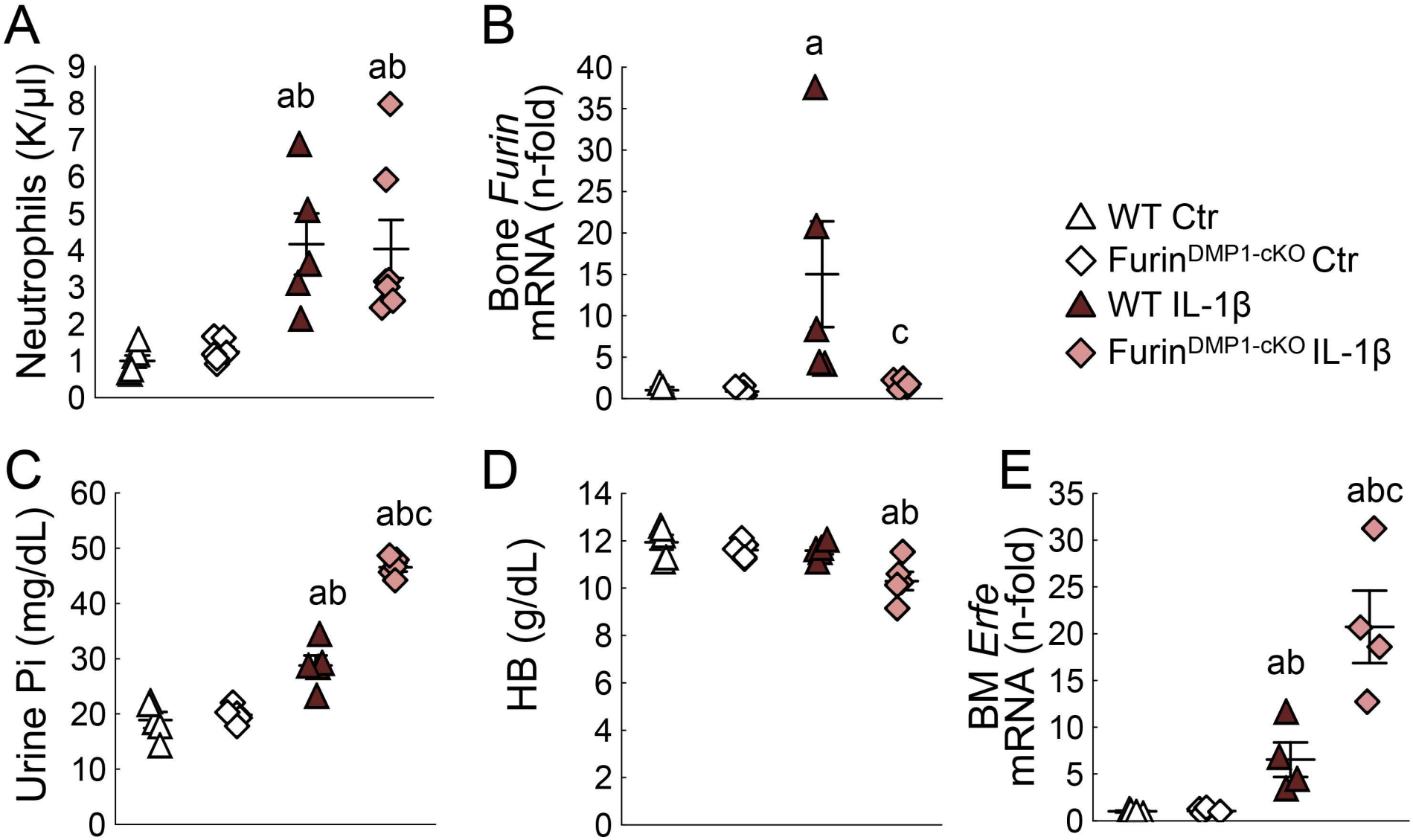

A
Neutrophils (K/µl)
0
1
2
3
4
5
6
7
8
9
ab
ab
B
Bone Furin mRNA (n-fold)
0
5
10
15
20
25
30
35
40
a
c
WT Ctr
Furin DMP1-cKO Ctr
WT IL-1β
Furin DMP1-cKO IL-1β
C
Urine Pi (mg/dL)
0
10
20
30
40
50
60
ab
abc
D
HB (g/dL)
0
2
4
6
8
10
12
14
ab
E
BM Erfe mRNA (n-fold)
0
5
10
15
20
25
30
35
ab
abc

Figure S5

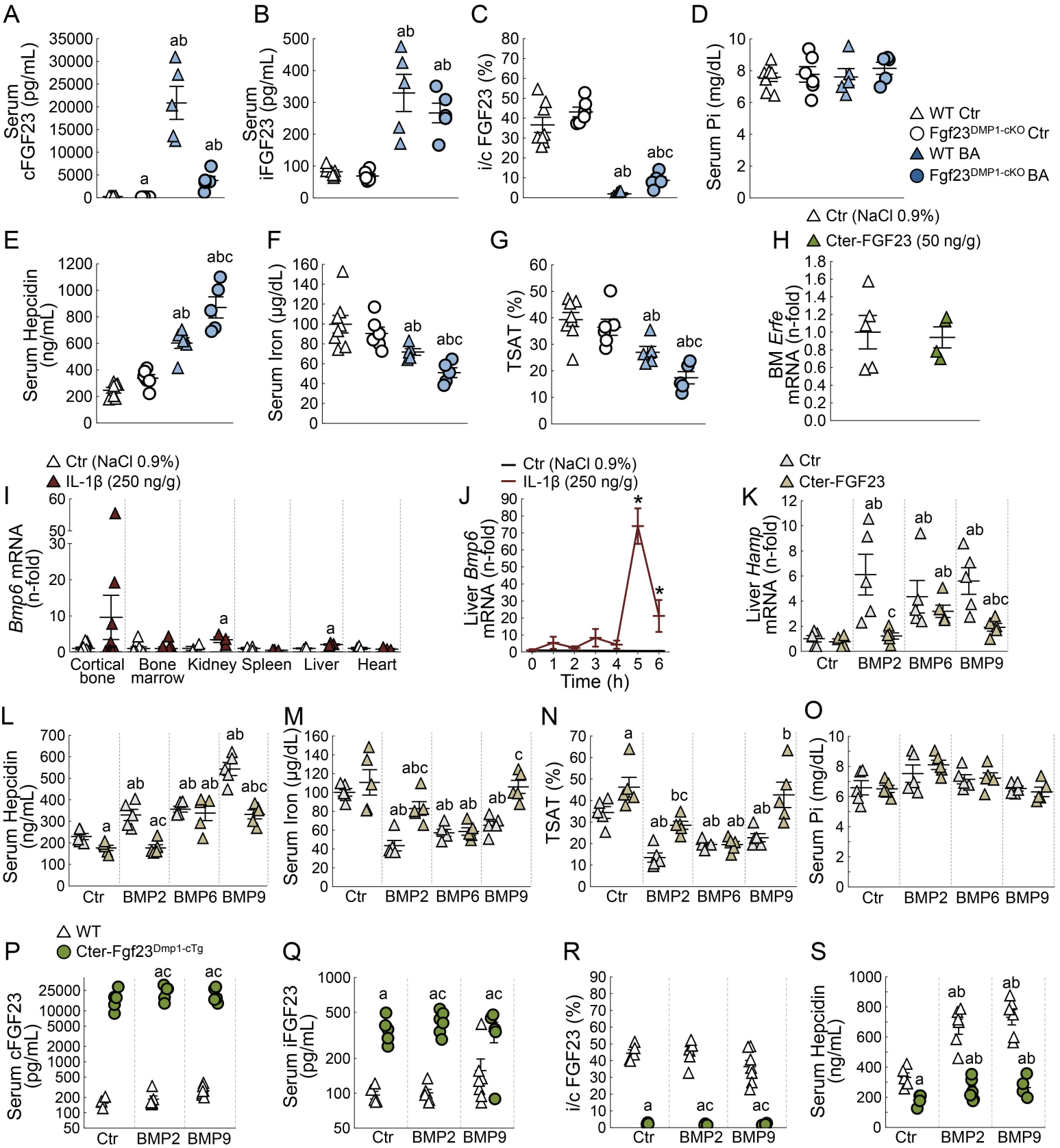
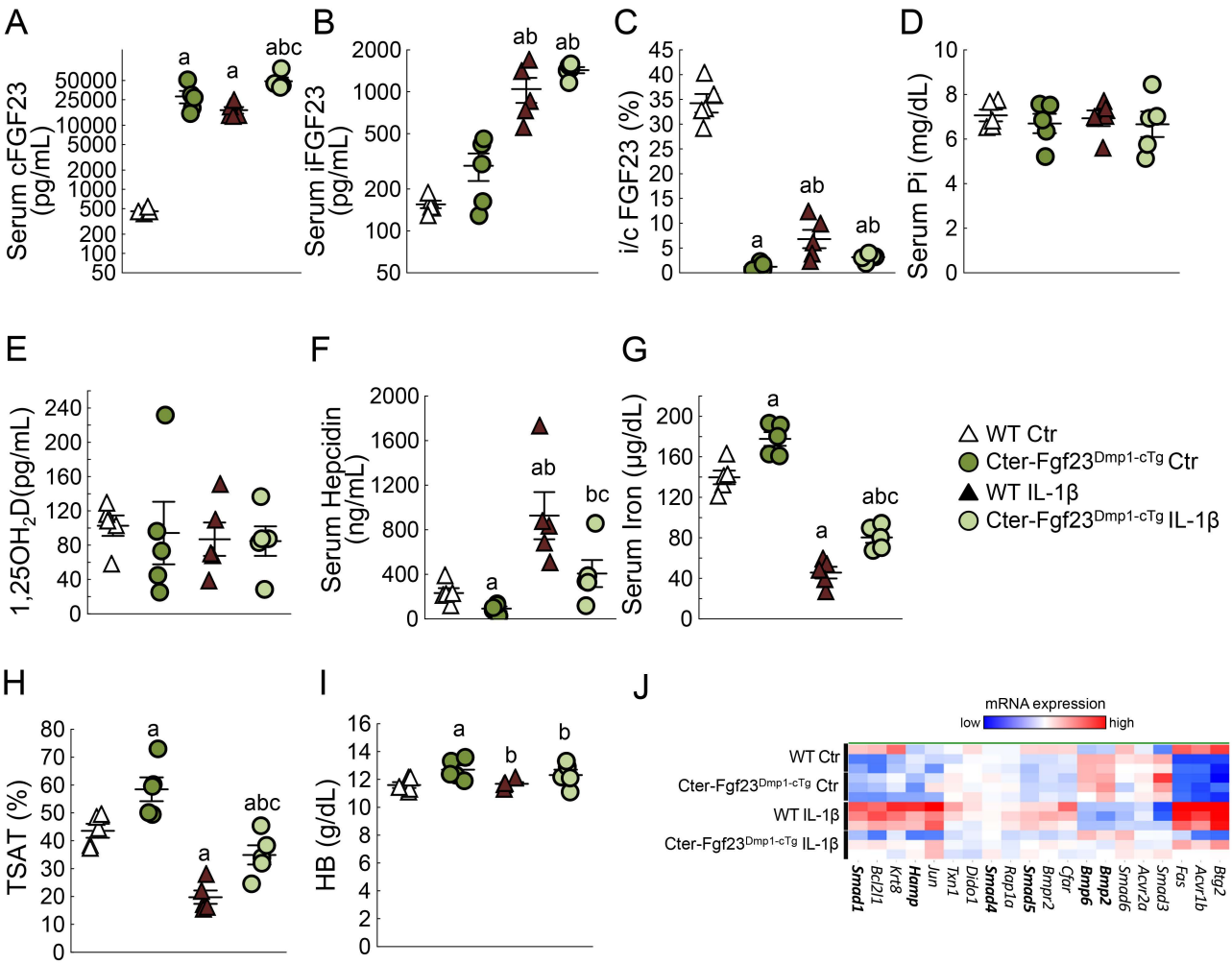

A
Serum cFGF23 (pg/mL)
B
Serum iFGF23 (pg/mL)
C
i/c FGF23 (%)
D
Serum Pi (mg/dL)
WT Ctr
Fgf23DMP1-cKO Ctr
WT BA
Fgf23DMP1-cKO BA
E
Serum Hepcidin (ng/mL)
F
Serum Iron (µg/dL)
G
TSAT (%)
H
BM Erfe mRNA (n-fold)
Ctr (NaCl 0.9%)
Cter-FGF23 (50 ng/g)
I
Ctr (NaCl 0.9%)
IL-1β (250 ng/g)
Bmp6 mRNA (n-fold)
Cortical bone
Bone marrow
Kidney
Spleen
Liver
Heart
J
Ctr (NaCl 0.9%)
IL-1β (250 ng/g)
Liver Bmp6 mRNA (n-fold)
Time (h)
K
Ctr
Cter-FGF23
Liver Hamp mRNA (n-fold)
Ctr
BMP2
BMP6
BMP9
L
Serum Hepcidin (ng/mL)
M
Serum Iron (µg/dL)
N
TSAT (%)
O
Serum Pi (mg/dL)
P
WT
Cter-Fgf23Dmp1-cTg
Serum cFGF23 (pg/mL)
Q
Serum iFGF23 (pg/mL)
R
i/c FGF23 (%)
S
Serum Hepcidin (ng/mL)

Figure S6


A
Serum cFGF23 (pg/mL)
50000
25000
10000
5000
2000
1000
500
200
100
50
a
a
abc
B
Serum iFGF23 (pg/mL)
2000
1000
500
200
100
50
ab
ab
C
i/c FGF23 (%)
45
40
35
30
25
20
15
10
5
0
a
ab
ab
D
Serum Pi (mg/dL)
10
8
6
4
2
0
E
1,25OH2D(pg/mL)
240
200
160
120
80
40
0
F
Serum Hepcidin (ng/mL)
2000
1600
1200
800
400
0
a
ab
bc
G
Serum Iron (µg/dL)
200
160
120
80
40
0
a
a
abc
WT Ctr
Cter-Fgf23Dmp1-cTg Ctr
WT IL-1β
Cter-Fgf23Dmp1-cTg IL-1β
H
TSAT (%)
80
70
60
50
40
30
20
10
0
a
a
abc
I
HB (g/dL)
16
14
12
10
8
6
4
2
0
a
b
b
J
mRNA expression
low
high
WT Ctr
Cter-Fgf23Dmp1-cTg Ctr
WT IL-1β
Cter-Fgf23Dmp1-cTg IL-1β
Smad1
Bcl2l1
Krt8
Hamp
Jun
Txn1
Dido1
Smad4
Rap1a
Smad5
Bmpr2
Cfar
Bmp6
Bmp2
Smad6
Acvr2a
Smad3
Fas
Acvr1b
Btg2